Food and Bioprocess Technology
https://doi.org/10.1007/s11947-023-03294-9

RESEARCH

Inline Determination of the Gel Elastic Modulus During Milk Coagulation Using a Multifiber Optical Probe

Zulma Villaquiran[1,2] · Anna Zamora[1] · Oscar Arango[1,2] · Manuel Castillo[1]

Received: 2 February 2023 / Accepted: 8 December 2023

Abstract

From a state-of-the-art point of view, it is currently possible to optically monitor the enzymatic coagulation of milk for real time estimation of the elastic modulus to cut the gel at optimum gel firmness. However, European cheese industry produces a wide variety of cheeses, many of them artisanal, and has a very fragmented productive structure with many small-, medium-sized companies. Therefore, if the technology is to be successfully uptake, it must be not only accurate but very low-cost. The objective of this work was to evaluate a low-cost commercial multifiber probe, for inline optical determination of curd firmness during cheese making. Preliminary tests were carried out to select the most appropriate fiber core size and wavelength and after that coagulation trials were performed following a fully randomized factorial design with two factors, i.e., concentration of protein (3.2, 3.6 and 4.0%) and added calcium (150, 200 and 250 mg L^{-1}), with three replicates. The observed linear increase of the least square means of the initial voltage with the protein content ($V_0 = 0.15[P, \%] + 0.88$; $R^2 = 0.999$), will be likely synergistic with the elastic modulus prediction if the model needs to be corrected for protein. Finally, the multifiber probe allowed predicting curd firmness using the proposed model with SEP values < 7 Pa. The present work has proven that a low-cost multifiber probe is suitable for accurate, real-time prediction of curd firmness during cheese manufacture.

Keywords Milk enzymatic coagulation · Light scattering · Elastic modulus · Multifiber probe · Curd firmness

Abbreviations

NIR	Near infrared
G'	Storage modulus
G''	Loss modulus
R	Light backscatter ratio
V_0	Initial voltage
ΔR	The increment of the backscatter profile during coagulation
R'	First derivative of R
R''	Second derivative of R
t_{max}	The elapsed time from enzyme addition to the first maximum of R'
t_{2max}	The elapsed time from enzyme addition to the first maximum of R″
t_{2min}	The elapsed time from enzyme addition to the first minimum of R″
$t_{G'1}$	Rheological gelation time (G' = 1 Pa)
$t_{G'30}$	Rheological cutting time (G' = 30 Pa)
t_{ag}	The duration of the aggregation phase ($t_{G'1}$—t_{max})
t_{F30}	Time required by the gel to strengthen from 1 to 30 Pa
tg δ_{30min}	Loss tangent at 30 min, calculated as tan δ = G''/G'
G'_{inf}	Value of the storage modulus at infinite time
G'_0	Value of the storage modulus at time at the beginning of gelationk_{GR}Constant representing the ratio between the rates of increase of G' and R values
R_{inf}	Asymptotic value at infinite time for the light scattering ratio, t = 45 min
R_0	R value at t_{2min}

✉ Manuel Castillo
manuel.castillo@uab.cat

[1] Centre d'Innovació, Recerca I Transferència en Tecnologia Dels Aliments (CIRTTA), TECNIO-CERTA-UAB, Departament de Ciència Animal I Dels Aliments, Facultat de Veterinària, Universitat Autònoma de Barcelona, 08193 Bellaterra, Spain

[2] Facultad de Ingeniería Agroindustrial, Universidad de Nariño, Ciudad Universitaria Torobajo, Pasto, Colombia

Published online: 15 January 2024

Introduction

In cheese manufacture, a simple and non-destructive technology for determining the right moment to cut the gel during rennet coagulation has been sought for a long time, with the aim of avoiding the use of subjective methods and to achieve a complete automation of the process (Arango et al., 2018a). Cutting time selection depends on the type of cheese produced and has a direct effect on product yield and quality. Early cutting, which enables great rearrangement of paracasein micelles, increases syneresis and reduces cheese moisture content, but increases fines amount, while late cutting has the opposite effects (Fagan et al., 2007). Therefore, cutting should be performed at a consistent curd firmness optimized for each type of cheese.

With the aim of objectively determine the cutting time during enzymatic milk coagulation, several methods have been studied but, most of them are intrusive, destructive, do not work inline or are not practical for in-plant implementation (O'Callaghan & O'Donnell, 2022). Changes of near infrared (NIR) light scattering during milk coagulation are directly related to the rate of aggregation and curd firming (Castillo, 2006; Castillo et al., 2003). Based on this, Castillo and Arango (2018) developed and patented a method for real-time monitoring of gel firmness (EP3036527 B1, 2018). This consists of a mathematical model that directly correlates NIR light scattering signal with the gel elastic modulus (G') and allows robust prediction of the rheological cutting time, i.e., when the gel reaches a specific firmness.

An optical fiber for spectroscopy consists of a core, a doped cladding, and a protective jacket. Considering that a separate illumination and collection channel minimizes background signals produced in the illumination fiber, initial research on the application of spectroscopy for the control of milk coagulation was performed with two-fiber sensors in which the distance between the source and the detector fibers were adjusted for an optimal intensity profile. Nowadays, multifiber probes with fiber core diameters of 50 to 600 µm are usually used in biomedical optical spectroscopy (Utzinger & Richards-Kortum, 2003). The probe is constituted by a central fiber and six surrounding fibers with illumination and collection interchangeable between them. Variations in scattering are due to inhomogeneities in the refractive index. Based on the fact that multiple readings reduce the noise by the square root of the number of readings, multiple collection fibers are being used for detecting both scattering and absorption properties of human tissues, which present great inhomogeneities, but can contain diagnostic information relevant to tissue pathology (Utzinger & Richards-Kortum, 2003). On the contrary, increasing the number of illumination fibers increases the sensitivity of the system but with the drawback of a greater background signal. Currently, a wide range of commercial multifiber probes is available at low to moderate prices.

Woodcock et al. (2008) reviewed the application of near- and mid-infrared spectroscopy as a useful tool for process monitoring, quality control, and authenticity determination in cheese processing and highlighted the potential of NIR spectroscopy for monitoring milk coagulation. On the other hand, Xie and Guo (2020) reviewed the measurement techniques such as integrating sphere, spatially resolved, frequency-domain, and time-resolved spectroscopes and calculation algorithms such as inverse adding double, Monte Carlo, and diffuse approximation to provide information for further studies on absorption and scattering properties of turbid foods.

The present study is different from the previous ones since it evaluates, for the first time, the use of a low-cost multifiber probe by monitoring both the evolution of the rheological elastic modulus and NIR light-scattering response of milk gels during enzymatic coagulation, according to the method patented by Arango and Castillo (2018), with the final objective of facilitating the implementation of this technology at an industrial level.

Materials and Methods

Preliminary Test: Multifiber Probe Selection

A preliminary test was performed to select a multifiber probe by comparing the VIS–NIR response during milk coagulation obtained with two commercial probes with a fiber core size of 400 µm (QR400-7-VIS-BX, Ocean Optics, Inc., Dunedin, FL, USA) and 600 µm (OCF-107982, Ocean Optics, Inc.), both with a probe ferrule diameter of ¼ inch (6.35 mm).

Both multifiber probes used had a 6-around-1 fiber bundle design, with the 6-fiber leg connecting to light emitting source and the single-fiber leg connecting to spectrophotometer. Under this configuration, light was transmitted by the six peripheral illumination fibers, and the central collection fiber transmitted the light backscattered at 180° by milk particles.

The tests were carried out using reconstituted low heat skim milk powder (whey protein nitrogen index of 6.0 mg g^{-1}, 32.5% protein, and 1.25% fat, Chr. Hansen SL, Jernholmen, Denmark; see "Milk Sample Preparation" section. for reconstitution procedure), which was standardized by mass balances at two concentrations of fat (0.5 and 3.6%) and protein (3.0 and 4.0%) with the skim milk powder and pasteurized cream extracted from fresh milk.

Coagulation tests were performed as follows: 20 mL milk samples were warmed up to 32 °C inside the measuring vat and 286 μL L^{-1} of a calcium chloride solution (525 g L^{-1} $CaCl_2$, Laboratorios Arroyo S.A., Santander, Spain) were added. When thermal equilibrium was reached, 110 μL L^{-1} of chymosin (CHY-MAX extra, 600 IMCU mL^{-1}, Chr. Hansen A/S, Hoersholsm, Denmark) was added. After vigorously stir for 30 s, the data capture system (see "Optical System to Monitor Enzymatic Coagulation Using a Multifiber Probe" section.) was started. Among all the wavelength bands generated as a function of time, those of 580, 680, 780, and 880 nm were analyzed since they comprise the range in which the enzymatic coagulation light backscatter profiles of milk provide the maximum response (Payne & Castillo, 2007).

Experimental Design

Once the probe with the best performance was selected, a complete randomized factorial design with two factors: protein concentration (3.2, 3.6, and 4.0%) and addition of anhydrous $CaCl_2$ (150, 200 and 250 mg L^{-1}), was used to evaluate the effect of these factors on light backscatter profile parameters during milk coagulation and to correlate them with the gel elastic modulus. The whole experiment was repeated three times (n = 3), giving a total of N = 27 trials. Milk coagulation (32 °C) was simultaneously monitored using the proposed optical system and a rheometer.

Milk Sample Preparation

As described for the preliminary test, low heat skim milk powder was reconstituted adjusting the protein levels by changing the amount of milk powder used, based on mass balances. Weighed milk powder was dissolved with distilled water at 45 °C and stirred for 20 min at ~ 500 rpm using a magnetic stirrer. Simultaneously, 286, 381 or 476 μL L^{-1} of the calcium chloride solution (525 g L^{-1} $CaCl_2$, Laboratorios Arroyo S.A.) were added. The reconstituted milk was left for 30 min at room temperature in the dark for complete rehydration of casein micelles.

Measurement of Ionic Calcium, pH, and Particle Size of Milk

Concentration of ionic calcium (Ca^{2+}) was determined in triplicate immediately after sample preparation using a Hach calcium-ion-selective electrode (ISE Ca^{2+} LZW9660C, Hach Company, Düsseldorf, Germany) incorporated into a Sension + multimeter (MM340, Hach Company). The calibration curve was daily performed with four standard solutions at 100, 150, 200, and 250 mg L^{-1} Ca^{2+} prepared from a stock solution at a calcium concentration of 1 g L^{-1} Ca^{2+}. The analysis was carried out following the equipment manufacturer's instructions.

The pH was also determined in triplicate at room temperature just after sample preparation by the potentiometric method, using a LZW5051T pH electrode coupled to a Sension + LPV2550T portable pH meter, both from Hach Company, with a resolution of 0.01 pH units. The electrode was calibrated with two buffer solutions of pH = 4.0 and pH = 7.0 before measurement, at the same temperature of the samples, following the manufacturer's instructions.

Particle size was analyzed in triplicate on samples refrigerated at ~ 4 °C, containing Thimerosal (Sigma-Aldrich, Buchs, Switzerland) as a preservative. Measurements were performed at room temperature (~ 20 °C). It was determined by dynamic light scattering using the Zetasizer Nano ZS particle size analyzer and its software version 7.11 (Malvern Instruments, Worcestershire, UK).

Optical System to Monitor Enzymatic Coagulation Using a Multifiber Probe

The optical system (Fig. 1) consisted of a tungsten halogen light source (LS-1, Ocean Optics, Inc.), a high-resolution spectrometer (HR4000, Ocean Optics, Inc.) with a detection range of 200 to 1100 nm coupled to a desktop computer, and a custom-made AISI 316L stainless steel measuring vat, all interconnected through the multifiber probe (see "Preliminary Test: Multifiber Probe Selection" section). The milk sample was introduced into the measuring vat, which had an oxidation treatment known as Nerinox, a diameter of 2.54 cm and a capacity of 20 mL. Coagulation temperature was kept at 32 °C by circulating water heated at 33.0 ± 0.1 °C (Ovantherm TC00, Suministros Grupo Esper, S.L., Barcelona, Spain) through the double wall of the vat (detail of the milk coagulation procedure is given in "Preliminary Test: Multifiber Probe Selection" section). Data acquisition was performed with an integration time of 200 ms and an average scan of 30 scans (OceanView 1.6.5, Ocean Optics, Inc.) giving one measurement every 6 s.

Subtraction of the corresponding dark spectrum was performed at each optical assay. The obtained light intensities were processed using the data processing software developed by Ctrl4Enviro S.L. (Barcelona, Spain) to obtain the light backscatter profile of each tested wavelength, as well as the optical parameters (see "Determination of Optical and Rheological Parameters" section).

Low-amplitude Oscillatory Rheology

A 40 mL aliquot from a milk sample at 32.00 ± 0.01 °C was deposited in the cup of RheoStress 1 (Thermo-Haake GmbH, Karlsruhe, Germany) rheometer for analysis.

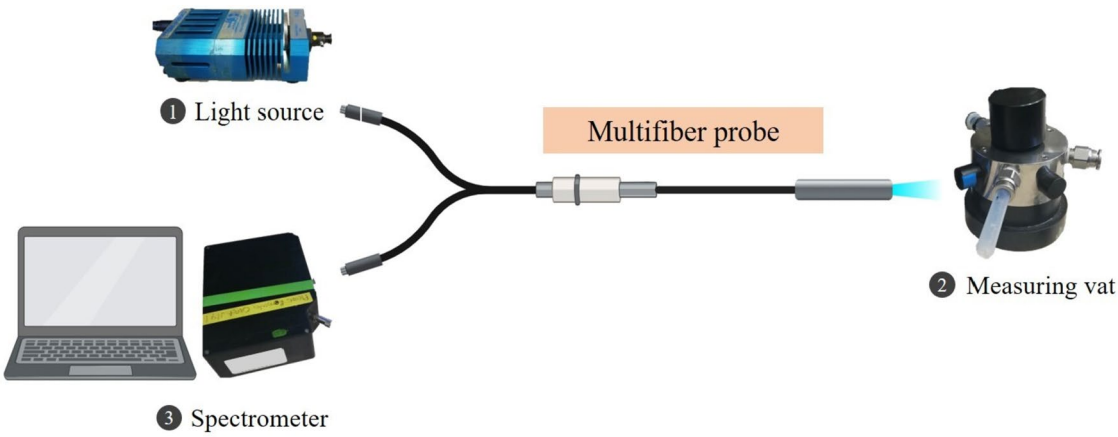

Fig. 1 Scheme of the optical system used to obtain the light scattering profile during enzymatic coagulation of milk using a multifiber probe

Measurements were performed using a cylindrical bob and cup geometry (Z34DIN). Strain and frequency were set up at 3% and 1 Hz, respectively. The enzyme was then added, and the mixture was stirred for 30 s (detail of the milk coagulation procedure and the experimental levels tested is given in "Preliminary Test: Multifiber Probe Selection" section and "Experimental Design" section, respectively). The coagulation process was monitored according to the procedure described by Arango and Castillo (2018). Rheological parameters measured were the storage modulus (G') and the loss modulus (G'').

Determination of Optical and Rheological Parameters

The light backscatter ratio (R) was calculated by dividing the recorded light intensity values by the average of the values obtained during the first minute of assay (i.e., initial voltage, V_0). The increment of the backscatter profile during coagulation (ΔR) was estimated as the difference between R at the end and at the beginning of coagulation. First (R') and second (R'') derivatives of R as a function of time were calculated. The elapsed times from enzyme addition to the first maxima of R' and R'' were defined as t_{max}, t_{2max}, respectively.

Rheological gelation time ($t_{G'1}$) and rheological cutting time ($t_{G'30}$) were defined as the time when the gels had G' values of 1 and 30 Pa, respectively. Parameter t_{max} indicates the end of the hydrolysis phase and the beginning of the aggregation phase (Arango et al., 2018b), while $t_{G'1}$ indicates the beginning of the gel firming phase. Thus, the duration of the aggregation phase (t_{ag}) was estimated as the difference between $t_{G'1}$ and t_{max}. Other identified parameters were t_{F30} (time required by the gel to strengthen from 1 to 30 Pa; i.e., $t_{G'30}$—$t_{G'1}$), and $tg\ \delta_{30min}$ (loss tangent calculated as $tan\ \delta = G''/G'$, with G' and G'' values obtained 30 min after enzyme addition).

Statistical Analysis

An analysis of variance (ANOVA) using the general linear model (GML) was conducted to identify the sources of variation for the physicochemical, optical, and rheological data. Protein and calcium concentrations, their interaction, and replication were introduced as factors in the model. The means of the variables with a significant effect of the factors were compared using Fisher's LSD test at a 5% probability level. Pearson's correlation was used to analyze the correlation between all the parameters evaluated. Analyses were carried out using MINITAB 18 statistical software (Minitab Inc., State College, Pennsylvania, USA).

To verify the fit of the model proposed by Arango and Castillo (2018) to predict rheological gel firmness values at the different experimental treatments, two out of three treatment replications were used to calibrate the model and obtain the regression coefficients, which were then used to validate the fit of the G' prediction model with the remaining independent replication. The same procedure was applied

Table 1 Analysis of variance and F statistics of the effect of added calcium, protein concentration, and their interaction on milk physicochemical parameters

Parameters	R^2	*F value*			
		P (DF = 2)	***AC*** (DF = 2)	***R*** (DF = 2)	***P*** × ***AC*** (DF = 4)
Ionic calcium	0.906	0.88^{ns}	0.52^{ns}	85.19^{***}	1.72^{ns}
pH	0.824	10.25^{**}	1.58^{ns}	17.02^{***}	0.16^{ns}
Particle size	0.884	98.05^{***}	1.64^{ns}	1.75^{ns}	3.32^{*}

$N = 27$, P protein concentration, AC added calcium, R replication, $P \times AC$ interaction between protein concentration and added calcium, *F value* ANOVA F-statistic, *DF* degree of freedom, R^2 coefficient of determination, *ns* not significant

$^{*}P < 0.05$; $^{**}P < 0.01$; $^{***}P < 0.001$

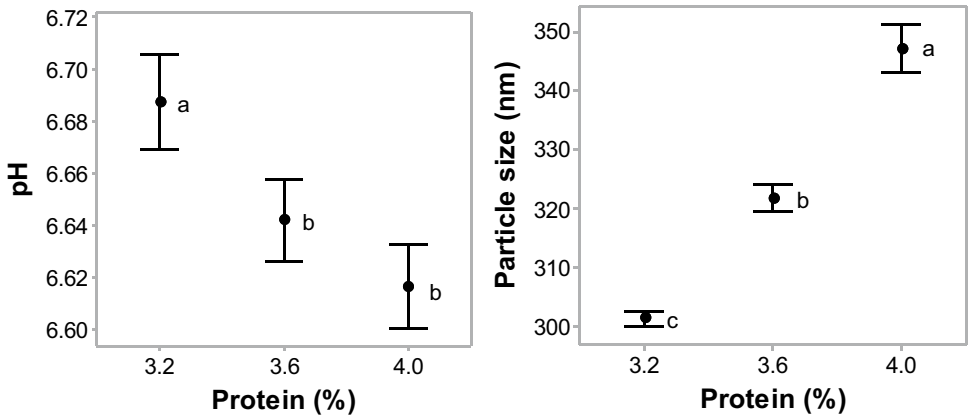

Fig. 2 Effect of protein on pH and particle size in reconstituted skim milk powder (N = 27; error bars correspond to standard deviations). Different letters (a, b, c) mean significant differences between protein levels ($P < 0.05$)

for the three possible replication combinations (1 and 2 – 3; 1 and 3 – 2; 2 and 3 – 1) and, the results were presented as average and standard deviation of the model fitting results. Additionally, a different method was introduced, which consisted in taking the averages of the *R versus* time profiles for the three replicates as reference. The calibration was performed using the two replications farthest from the average profile, and the validation using the remaining one.

For each calibration, regression coefficients, which were obtained with the Excel 2016 Solver tool (Microsoft

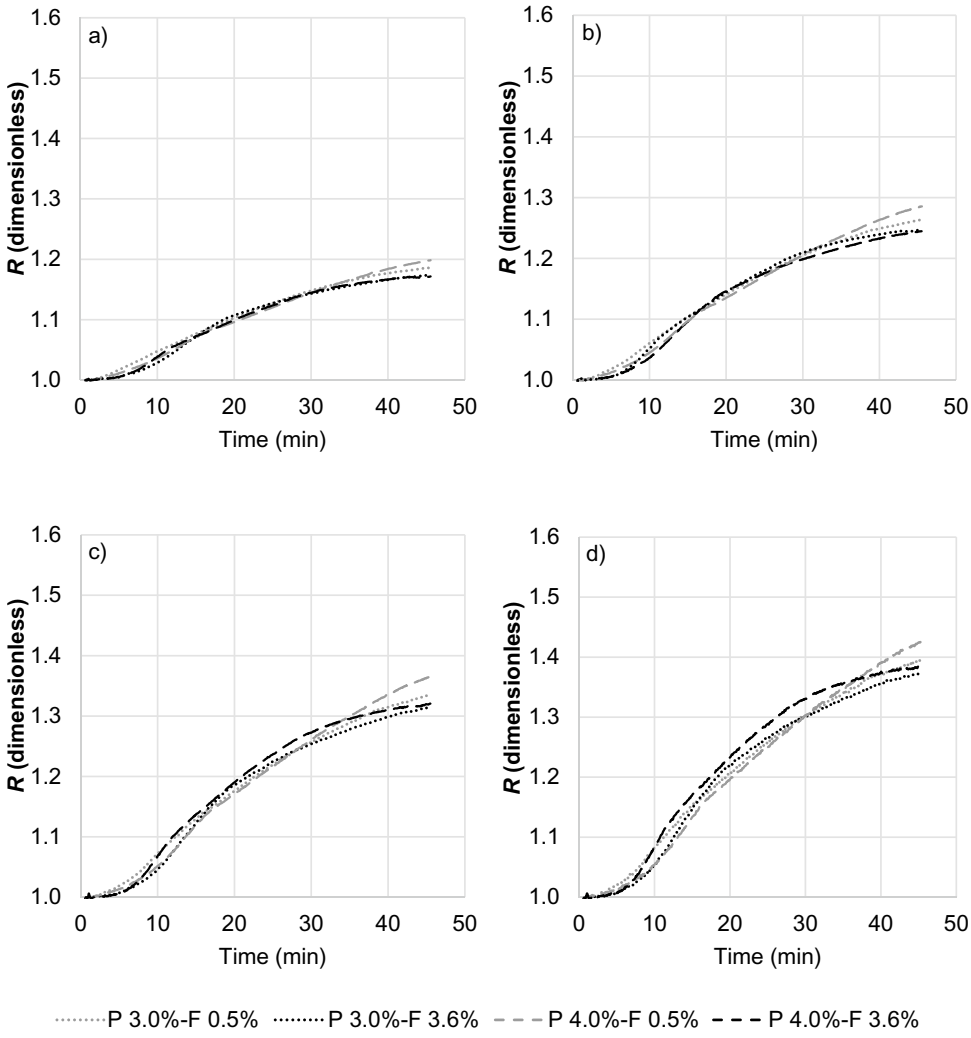

Fig. 3 Effect of fat (F) and protein (P) concentration on milk coagulation light backscatter ratio profiles obtained using a 400 µm multifiber probe. **a** 580 nm; **b** 680 nm; **c** 780 nm; **d** 880 nm

Corporation, Redmond, USA), were analyzed using ANOVA. The prediction model described by Arango and Castillo (2018) has five parameters: G'_{inf} (value of the storage modulus at infinite time), G'_0 (value of the storage modulus at the beginning of gelation; this parameter was not fitted, it was assumed to be 5 Pa) k_{GR} (constant representing the ratio between the rates of increase of G' and R values), R_{inf} (asymptotic value at infinite time for the light scattering ratio, t = 45 min) and R_0 (R value at t_{2min}). The four fitted parameters are hereafter shown randomly coded with the letters a, b, c, and d, due to confidentiality reasons. The coefficient of determination (R^2), standard error of prediction (SEP), and coefficient of variation (CV) were determined to evaluate the model performance, i.e., the fit between the G' values measured with the rheometer and those obtained with the model.

Results and Discussion

Effect of Protein Concentration and Added Calcium on pH, Ionic Calcium, and Particle Size of Milk Samples

According to the ANOVA (Table 1), the level of added calcium had no significant effect on the physicochemical parameters evaluated ($P > 0.05$), while pH and particle size values varied significantly as a function of protein levels ($P < 0.01$; $P < 0.001$). Significant differences were found for particle size due to protein and added calcium interaction ($P < 0.05$), indicating that the change of particle size in milk with the protein level depend on the calcium added. Indeed, significant Pearson's correlation coefficients were observed between protein concentration and pH (r = -0.91) and particle size (r = 0.96). Previous studies have shown that the addition of $CaCl_2$ to milk has effects on Ca^{2+} and pH (Lewis, 2011). According to Walstra et al. (2006) and Fox et al. (2017), when $CaCl_2$ is added to milk, Ca^{2+} increases approximately by 30% and about 40% goes into the micelle displacing protons and reducing pH. However, this was not evident in the present study, probably because the levels of added $CaCl_2$ were not high enough.

As expected, pH of the samples significantly decreased with increasing protein concentration from 3.2 to 3.6% (Fig. 2). This is related to the fact that when milk is concentrated to obtain milk powder during dehydration processing at an industrial plant, the soluble phase, which is saturated with calcium, is concentrated and the excess calcium moves into the micellar phase as colloidal calcium phosphate. When calcium moves into the micelle in combination with phosphate, protons are released, and consequently, pH decreases. The following equation represents the equilibrium between Ca^{2+} and colloidal calcium phosphate (Lin et al., 2006):

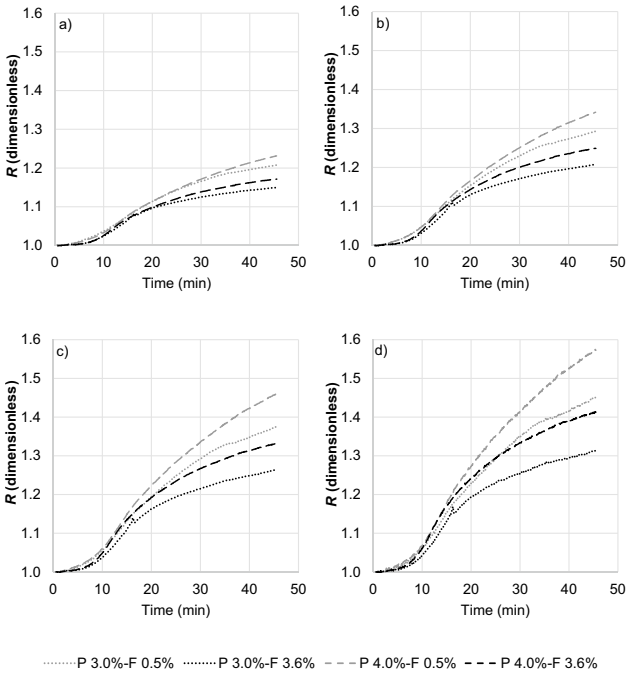

Fig. 4 Effect of fat (F) and protein (P) concentration on milk coagulation light backscatter ratio profiles obtained using a 600 µm multifiber probe. **a** 580 nm; **b** 680 nm; **c** 780 nm; **d** 880 nm

$$3Ca^{2+} + 2HPO_4^{2-} \leftrightarrow Ca_3(PO_4)_2 + 2H^+$$

That is, likely, how pH of the aqueous phase of the experimental samples is reduced by increasing the amount of milk powder needed to reach the required protein level.

The particle size associated with casein micelles in skimmed milk significantly increased with higher protein levels (Fig. 2). As previously explained, pH significantly decreased when protein increased, promoting the release of micellar calcium into the aqueous phase, and displacing the equilibrium to the left in the above equation. Therefore,

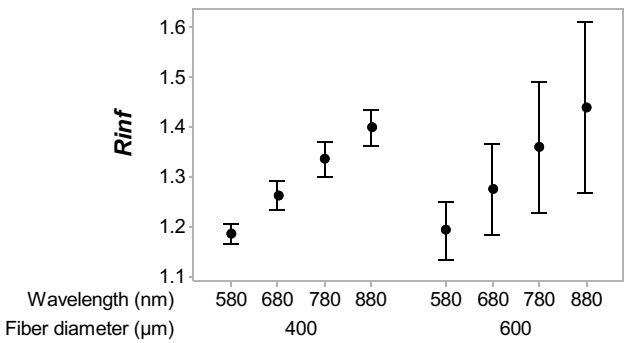

Fig. 5 Effect of fiber core size and wavelength on the asymptotic value at infinite time for the light scattering ratio (R_{inf}) (N = 4; error bars correspond to standard deviations of the four tested conditions: 3.0 and 4.0% protein, and 0.5 and 3.6% fat)

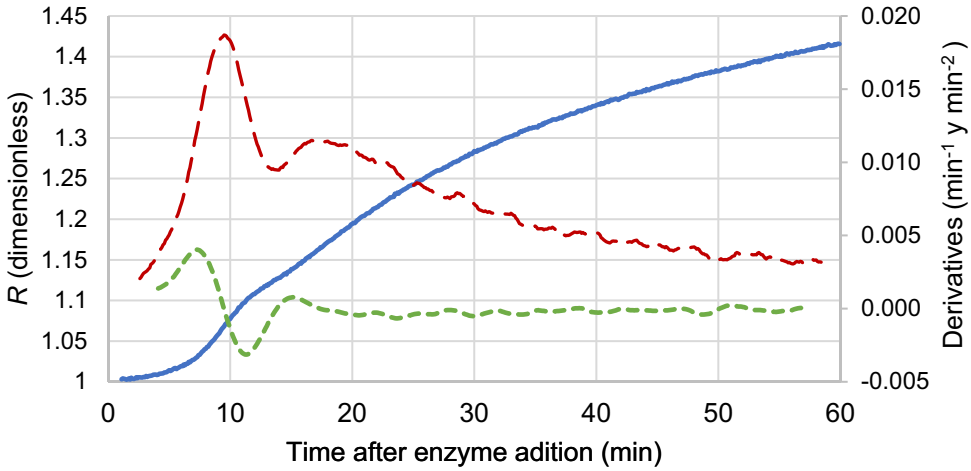

Fig. 6 Light scattering profile obtained during enzymatic coagulation of milk (protein 4.0%; $CaCl_2$ 250 mg L^{-1}) using a 600 µm multifiber probe at 780 nm. Blue: light backscatter ratio (R); red: first derivative (R'); green: second derivative (R'')

colloidal calcium phosphate that maintains the micelles intact is dissolved, resulting in a reduction in the strength and number of bonds, and consequently, the micelles are swollen (Walstra et al., 2006).

Multifiber Probe Selection

The comparison of light backscatter profiles showed that the increment of the backscatter profile during coagulation (ΔR) increased slightly with the 600 µm-core probe and with increasing wavelength (Figs. 3 and 4). High values in ΔR (at a constant time) are related to shorter coagulation times, as previous studies have shown (Arango et al., 2018a; Salvador et al., 2019). ΔR increased at high protein levels but decreased as the fat concentration increased for the two probes evaluated (Figs. 3 and 4). That is because casein micelles are much smaller than fat globules, and the water/casein refraction index difference is smaller than that for water/fat and, consequently, casein micelles backscatter less light (Castillo et al., 2005). Fat generates greater light backscattering and thereby a significantly higher V_0. Therefore, since R is calculated as the ratio between the voltage at time t and V_0, the relative increase in R is lower in samples with more fat and so is the value of ΔR as can be observed clearly in Fig. 4.

The 600 µm-core probe showed a higher mean R_{inf} value than the 400 µm probe and a higher deviation associated with a greater separation between curves (Fig. 5). Therefore, this probe was more sensitive to protein and fat levels. But its light backscatter profiles at the longest wavelength (880 nm) showed too much noise (Fig. 4d). That is why the 600 µm-core probe at 780 nm (Fig. 4c) was selected for the main experiment.

Effect of Calcium Chloride and Protein Concentration on Optical and Rheological Parameters of Milk Coagulation

Data obtained using the selected multifiber probe to monitor milk coagulation (Fig. 6) showed that both light scatter profiles and resulting derivatives were like those obtained

Table 2 ANOVA and F statistics of the effect of protein, $CaCl_2$ and their interaction on optical and rheological parameters during enzymatic coagulation of milk

Parameter	R^2	*F* value		
		P (DF = 2)	*AC* (DF = 2)	*P*×*AC* (DF = 4)
V_0	0.799	31.03^{***}	2.71^{ns}	0.99^{ns}
t_{max}	0.723	2.75^{ns}	11.41^{**}	4.67^{**}
t_{2max}	0.695	6.31^{**}	8.89^{**}	2.67^{ns}
$t_{G'1}$	0.570	5.42^{*}	4.16^{*}	1.18^{ns}
$t_{G'30}$	0.888	59.95^{***}	6.5^{**}	2.5^{ns}
t_{ag}	0.534	6.64^{**}	0.95^{ns}	1.35^{ns}
t_{F30}	0.939	126.78^{***}	6.18^{**}	3.16^{*}
$tg\ \delta_{30min}$	0.695	11.32^{**}	4.31^{*}	2.45^{ns}

$N = 27$, P protein concentration, AC added calcium, $P \times AC$ interaction between protein concentration and added calcium, F *value* ANOVA F-statistic, DF degree of freedom, R^2 coefficient of determination, V_0 initial voltage, t_{max} elapsed time from enzyme addition to the first maximum of backscatter-ratio first derivative; t_{2max}, elapsed time from enzyme addition to the first maximum of backscatter-ratio second derivative, $t_{G'1}$ rheological gelation time when $G' = 1$ Pa, $t_{G'30}$ rheological gelation time when $G' = 30$ Pa, t_{ag} duration of the aggregation phase, t_{F30} time required by the gel to strengthen from 1 to 30 Pa, $tg\ \delta_{30min}$ loss tangent calculated as $tan\ \delta = G''/G'$, with G' and G'' values obtained 30 min after enzyme addition, *ns* not significant

$^{*}P < 0.05$; $^{**}P < 0.01$; $^{***}P < 0.001$

Table 3 Mean comparison of optical and rheological parameters obtained during enzymatic coagulation, as a function of protein concentration (%)

Protein	V_0	t_{max}	t_{2max}	$t_{G'1}$	$t_{G'30}$	t_{ag}	t_{F30}	$tg\ \delta_{30min}$
3.2	1.348^{c}	9.9^{b}	7.3^{b}	19.1^{a}	49.7^{a}	9.2^{a}	30.6^{a}	0.277^{a}
3.6	1.409^{b}	10.1^{ab}	7.7^{ab}	19.6^{a}	42.0^{b}	9.5^{a}	22.3^{b}	0.277^{a}
4.0	1.465^{a}	10.5^{a}	8.1^{a}	17.0^{b}	31.8^{c}	6.5^{b}	14.9^{c}	0.270^{b}

Means with same letters are not significantly different using Fisher's test at $P<0.05$; number of replications = 3; number of observations, N = 27

V_0 initial voltage (V), t_{max} elapsed time from enzyme addition to the first maximum of backscatter-ratio first derivative (min), t_{2max} elapsed time from enzyme addition to the first maximum of backscatter-ratio second derivative (min), $t_{G'1}$ rheological gelation time when $G'=1$ Pa (min), $t_{G'30}$ rheological gelation time when $G'=30$ Pa (min), t_{ag} duration of the aggregation phase (min), t_{F30} time required by the gel to strengthen from 1 to 30 Pa (min), $tg\ \delta_{30min}$ loss tangent calculated as $tan\ \delta=G''/G'$, with G' and G'' values obtained 30 min after enzyme addition (dimensionless)

with other devices in previous studies (Arango et al., 2015; Fagan et al., 2007; Salvador et al., 2019).

Figure 6 shows how to obtain information related to the phases of enzymatic coagulation, as it was explained in "Determination of Optical and Rheological Parameters" section. For example, t_{max} and t_{2max} values refer to the times from the addition of the enzyme to the first maximum values of the first (R') and second (R'') derivatives respectively. These parameters have shown to have a strong correlation with the moment when the hydrolysis phase ends and the aggregation phase begins (Arango et al., 2018b).

Therefore, it is possible to determine the optical parameters and analyze their behavior like has been done in previous works. The increase in the light scatter ratio ranged from 27 to 35% after 45 min, which is in the range reported for cow's milk (Nicolau et al., 2015). ANOVA for the effect of protein and $CaCl_2$ on optical and rheological parameters (Table 2), showed that protein concentration significantly affected the optical parameters V_0 ($P<0.001$) and t_{2max} ($P<0.01$), as well as all the rheological parameters. In addition, strong correlations were found between protein concentration and V_0, $t_{G'30}$ and t_{F30} with Pearson's coefficients of 0.93, -0.91, and -0.95, respectively. Optical parameters, except for V_0, and rheological parameters, except for t_{ag}, were affected by added $CaCl_2$, probably because of the concomitant pH decrease. Furthermore, the ANOVA revealed a significant effect of the protein and added calcium interaction on t_{max} ($P<0.01$) and t_{F30} ($P<0.05$). Therefore, the difference of these parameters with the increase of protein depends on the calcium added.

A significant and linear increase of V_0 was observed with increasing protein concentration (Table 3). In addition, the optical parameter t_{2max} showed significant differences between 3.2% and 4.0% ($P<0.05$). This indicates that the increase in the protein level caused a delay in the hydrolysis phase and, consequently, delayed the beginning of the micellar aggregation phase. This is attributed to the fact that at protein concentrations higher than 3% a decrease in the enzyme/casein ratio occurs, causing enzyme saturation by the substrate. Thus, a longer time is required to generate sufficient hydrolysis of the κ-casein and induce micelle aggregation (Fox et al., 2017; Salvador et al., 2019).

Increasing protein from 3.2 to 3.6% significantly decreased the rheological parameters $t_{G'30}$ and t_{F30}. Also, when protein was increased from 3.6 to 4.0% all rheological parameters ($t_{G'30}$, t_{F30}, $t_{G'1}$, t_{ag} and $tg\ \delta_{30min}$) decreased significantly ($P<0.05$). These results are in agreement with those observed by Arango et al. (2018b) and Salvador et al.

Table 4 Mean comparison of optical and rheological parameters obtained during enzymatic coagulation, as a function of added $CaCl_2$ (mg L^{-1})

$CaCl_2$	V_0	t_{max}	t_{2max}	$t_{G'1}$	$t_{G'30}$	t_{ag}	t_{F30}	$tg\ \delta_{30min}$
150	1389.7^{b}	10.9^{a}	8.2^{a}	20.0^{a}	44.4^{a}	9.1^{a}	24.5^{a}	0.278^{a}
200	1407.3^{ab}	9.8^{b}	7.4^{b}	18.0^{b}	40.3^{b}	8.2^{a}	22.3^{b}	0.274^{b}
250	1424.4^{a}	9.8^{b}	7.5^{b}	17.7^{b}	38.7^{b}	7.9^{a}	21.1^{b}	0.273^{b}

Means with same letters are not significantly different using Fisher's test at $P<0.05$; number of replications = 3; number of observations, N = 27

V_0 initial voltage (V), t_{max} elapsed time from enzyme addition to the first maximum of backscatter-ratio first derivative (min), t_{2max} elapsed time from enzyme addition to the first maximum of backscatter-ratio second derivative (min), $t_{G'1}$ rheological gelation time when $G'=1$ Pa (min), $t_{G'30}$ rheological gelation time when $G'=30$ Pa (min), t_{ag} duration of the aggregation phase (min), t_{F30} time required by the gel to strengthen from 1 to 30 Pa (min), $tg\ \delta_{30min}$ loss tangent calculated as $tan\ \delta=G''/G'$, with G' and G'' values obtained 30 min after enzyme addition (dimensionless)

Table 5 Analysis of variance and *F* statistics of the effect of protein, added calcium and their interaction on the parameters of the *G′* prediction model proposed by Arango and Castillo (2018)

Parameter	R^2	*F value*		
		P (DF = 2)	***AC*** (DF = 2)	***P*** × ***AC*** (DF = 4)
a	0.672	9.84^{**}	4.47^{*}	2.09^{ns}
b	0.590	6.38^{**}	4.32^{*}	1.13^{ns}
c	0.969	264.76^{***}	0.31^{ns}	6.71^{**}
d	0.931	104.36^{***}	8.9^{**}	4.33^{*}

a, b, c and *d*, parameters of the prediction model

N = 27, *P* protein concentration (3.2, 3.6 and 4.0%), *AC* added calcium (150, 200 and 250 mg L^{-1}), *P* × *AC* interaction between protein concentration and added calcium, *F value,* ANOVA F-statistic, *DF* degree of freedom, R^2 coefficient of determination, *ns* not significant

$^{*}P<0.05$; $^{**}P<0.01$; $^{***}P<0.001$

(2019), who attributed this behavior to the increase in the number of collisions between para-κ-casein residues due to a reduction of the average distance between micelles as protein concentration increases, accelerating the two main phases of gel formation (micellar aggregation and firmness development). The parameter $tg\ \delta_{30min}$ decreased significantly at high protein levels ($P<0.05$), resulting in stronger gels with less tendency to syneresis, as explained by Arango et al. (2015)

Addition of $CaCl_2$ from 150 to 200 mg L^{-1} caused a significant decrease of t_{max}, t_{2max}, $t_{G'1}$, $t_{G'30}$, and t_{F30} (Table 4; $P<0.05$). But $CaCl_2$ increment to 250 mg L^{-1} did not induce any further effect.

As previously stated, $CaCl_2$ addition to milk generates an increase in ionic and colloidal calcium, which is associated with a decrease in pH, increasing the rate of the hydrolysis, gel formation, and gel firmness phases with the reduction in the associated parameters t_{max}, $t_{G'30}$, and t_{F30}, respectively. The decrease in $tg\ \delta_{30min}$ values is related to an increment in gel firmness due to the addition of $CaCl_2$. The results are consistent with those obtained by Arango et al. (2015).The decrease in pH also generates a reduction in the intermicellar electrostatic repulsion, since it neutralizes the net negative charge of micelles increasing the attraction between them and accelerating gelation (Sandra et al., 2012).

Finally, significant Pearson's correlations ($P<0.05$) were observed among optical and rheological parameters with $0.73<r<0.98$ and $0.68<r<0.99$, respectively. In addition, between optical and rheological parameters, strong correlations were evident between V_0 and $t_{G'30}$ ($r=-0.88$) and t_{F30} ($r=-0.91$), indicating that the higher the protein, the higher the V_0 and the shorter the hardening times.

G′ Prediction Model: Parameters, Calibration and Validation

ANOVA presented in Table 5 shows the effect of protein and added $CaCl_2$ on the parameters of the model proposed by Arango and Castillo (2018) for elastic modulus (*G′*) prediction during enzymatic coagulation of milk, using *R* values. *F* values for protein concentration were considerably higher than those for $CaCl_2$, due to the mentioned effect of proteins on gel firmness. As can be seen in the ANOVA, there were significant differences in all parameters of the model among protein levels ($P<0.01$). Calcium added had the same behavior ($P<0.05$), except in parameter *c* ($P>0.05$). Parameters *c* and *d* showed significant interaction between the variables protein and added calcium ($P<0.05$). Therefore, the evolution of *c* and *d* with the increase of protein depend on the added calcium.

Parameters *a* and *b* significantly decreased at the highest tested protein concentration (Table 6; $P<0.05$). Parameter *c* decreased with increasing protein concentration, whereas the opposite occurred with *d*. The effect of protein and $CaCl_2$ on the parameters of the model showed a consistent response, which is expected to be aligned with changes on the aggregation and firming phases of enzymatic coagulation, as well as with gel firmness. As a result, it seems feasible to account for the effect of both protein and $CaCl_2$ by appropriate adjustment of the regression coefficients.

Table 6 Mean comparison of the parameters of the *G′* prediction model, as a function of protein concentration (%) and added $CaCl_2$ (mg L^{-1})

Parameter	Protein			R^2	$CaCl_2$			R^2
	3.2	**3.6**	**4.0**		**150**	**200**	**250**	
a	1.40^{a}	1.38^{a}	1.35^{b}	0.987	1.40^{a}	1.37^{ab}	1.36^{b}	0.923
b	1.21^{a}	1.22^{a}	1.18^{b}	0.519	1.22^{a}	1.19^{b}	1.19^{b}	0.750
c	131.99^{a}	122.14^{b}	113.35^{c}	0.999	122.86^{a}	122.38^{a}	122.25^{a}	0.901
d	0.22^{c}	0.26^{b}	0.35^{a}	0.953	0.26^{b}	0.28^{a}	0.29^{a}	0.964

Means within same row with same letters are not significantly different using Fisher's test at $P<0.05$; number of replications = 3; number of observations, N = 27. R^2, coefficient of determination. ***a***, ***b***, ***c*** and ***d***, parameters of the prediction model

Table 7 Model performance indicators obtained at different protein concentrations and added calcium. Results for three calibrations and three validations per treatment

Treatment		Calibration[a]					Validation[b]				
P	*AC*	G'_{obs}	G'_{pred}	R^2	SEP	CV	G'_{obs}	G'_{pred}	R^2	SEP	CV
3.2	150	30.0	30.2	0.9998	0.19	0.9	30.1	34.7	0.9949	10.51	52.5
3.2	200	30.1	29.9	0.9996	0.39	1.9	30.1	31.2	0.9996	9.14	45.6
3.2	250	30.0	30.0	0.9998	0.18	0.9	30.1	30.3	0.9994	3.06	15.3
3.6	150	30.1	30.1	0.9995	0.32	1.6	30.1	34.9	0.9869	13.63	67.9
3.6	200	30.0	30.0	0.9997	0.20	1.0	30.0	30.4	0.9976	2.06	10.3
3.6	250	30.0	29.6	0.9997	0.21	1.0	30.0	29.8	0.9996	2.96	14.8
4	150	30.1	30.3	0.9997	0.23	1.1	30.1	33.8	0.9977	11.18	55.6
4	200	30.0	30.2	0.9997	0.22	1.1	30.1	30.0	0.9996	2.27	11.3
4	250	30.0	30.0	0.9998	0.17	0.8	30.0	30.8	0.9997	6.31	31.4
Average		*30.1 ± 0.0*	*30.0 ± 0.2*	*0.9997*	*0.23*	*1.2*	*30.1 ± 0.0*	*31.8 ± 2.1*	*0.9972*	*6.79*	*33.8*

P protein concentration (%), *AC* added calcium (mg·L^{-1}), R^2 coefficient of determination, *SEP* standard error of prediction (Pa), *CV* coefficient of variation (%), G'_{obs} and G'_{pred} values of observed and predicted, G' when observed $G' \approx 30$ Pa, respectively, *Number of experiments* N = 27, N_c Number of datapoints for each calibration, $244 < N_c < 736$, N_v Number of datapoints for each validation, $118 < N_v < 388$

[a]Each calibration was performed with data from two replications in a range of G' between 5 and 30 Pa. Values correspond to means of the three possible calibrations per treatment (see "Statistical Analysis" section) with standard deviations ranging from 0.0 to 0.4 Pa

[b]Each validation was performed with the data from the independent replication not used in the calibration set. Values correspond to means of the three possible validations per treatment (see "Statistical Analysis" section) with standard deviations ranging from 0.0 to 23.9 Pa

Calibrations performed with the three replicas in all possible combinations showed a good fit of the data, with SEP and CV lower than 0.4 Pa and 2%, respectively (Table 7). Note that uncertainty of the rheological G´ measurements was ~ 0.5 Pa. For the validation, SEP and CV values ranged from 2.06 to 13.63 Pa and from 10.3 to 55.6%, respectively. The predictive models were able to explain between 98.7 and 99.9% of the variation of predicted G' when observed

Table 8 Model performance indicators obtained at different protein concentrations and added calcium. Results for two calibrations and one validation per treatment

Treatment		Calibration[a]					Validation[b]				
P	*AC*	G'_{obs}	G'_{pred}	R^2	SEP	CV	G'_{obs}	G'_{pred}	R^2	SEP	CV
3.2	150	30.1	30.2	0.9997	0.20	1.0	30.1	34.4	0.9992	3.33	16.6
3.2	200	30.1	30.0	0.9996	0.33	1.7	30.0	38.0	0.9993	6.89	34.4
3.2	250	30.0	30.0	0.9998	0.18	0.9	30.1	32.6	0.9979	2.06	10.4
3.6	150	30.1	30.2	0.9996	0.30	1.5	30.1	25.0	0.9994	4.00	20.0
3.6	200	30.0	30.0	0.9997	0.21	1.0	30.0	32.1	0.9876	1.86	9.3
3.6	250	30.0	29.6	0.9997	0.20	1.0	30.1	31.9	0.9989	1.06	5.3
4	150	30.1	30.2	0.9997	0.22	1.1	30.1	29.7	0.9980	1.06	5.3
4	200	30.0	30.2	0.9997	0.21	1.0	30.2	31.9	0.9993	1.53	7.6
4	250	30.0	30.0	0.9998	0.17	0.8	30.0	33.0	0.9996	2.35	11.7
Average		*30.1 ± 0.0*	*30.0 ± 0.2*	*0.9997*	*0.22*	*1.1*	*30.1 ± 0.1*	*32.1 ± 3.5*	*0.9989*	*2.68*	*13.4*

P protein concentration (%), *AC* added calcium (mg·L^{-1}), R^2 coefficient of determination, *SEP* standard error of prediction (Pa), *CV* coefficient of variation (%), G'_{obs} and G'_{pred}, values of observed and predicted G' when observed $G' \approx 30$ Pa, respectively, *Number of experiments* N = 27, N_c, Number of datapoints for each calibration, $244 < N_c < 657$, N_v, Number of datapoints for each validation, $130 < N_v < 388$

[a]Each calibration was performed with data from the two replications of the curve R *vs* time farthest to the average, in a range of G' between 5 and 30 Pa. Values correspond to the only possible calibration per treatment (see "Statistical Analysis" section) with standard deviations ranging from 0.0 to 0.5 Pa

[b]Each validation was performed with data from the replication of the curve R *vs* time closest to the average, not used in the calibration set. Values correspond to the only possible validation per treatment (see "Statistical Analysis" section)

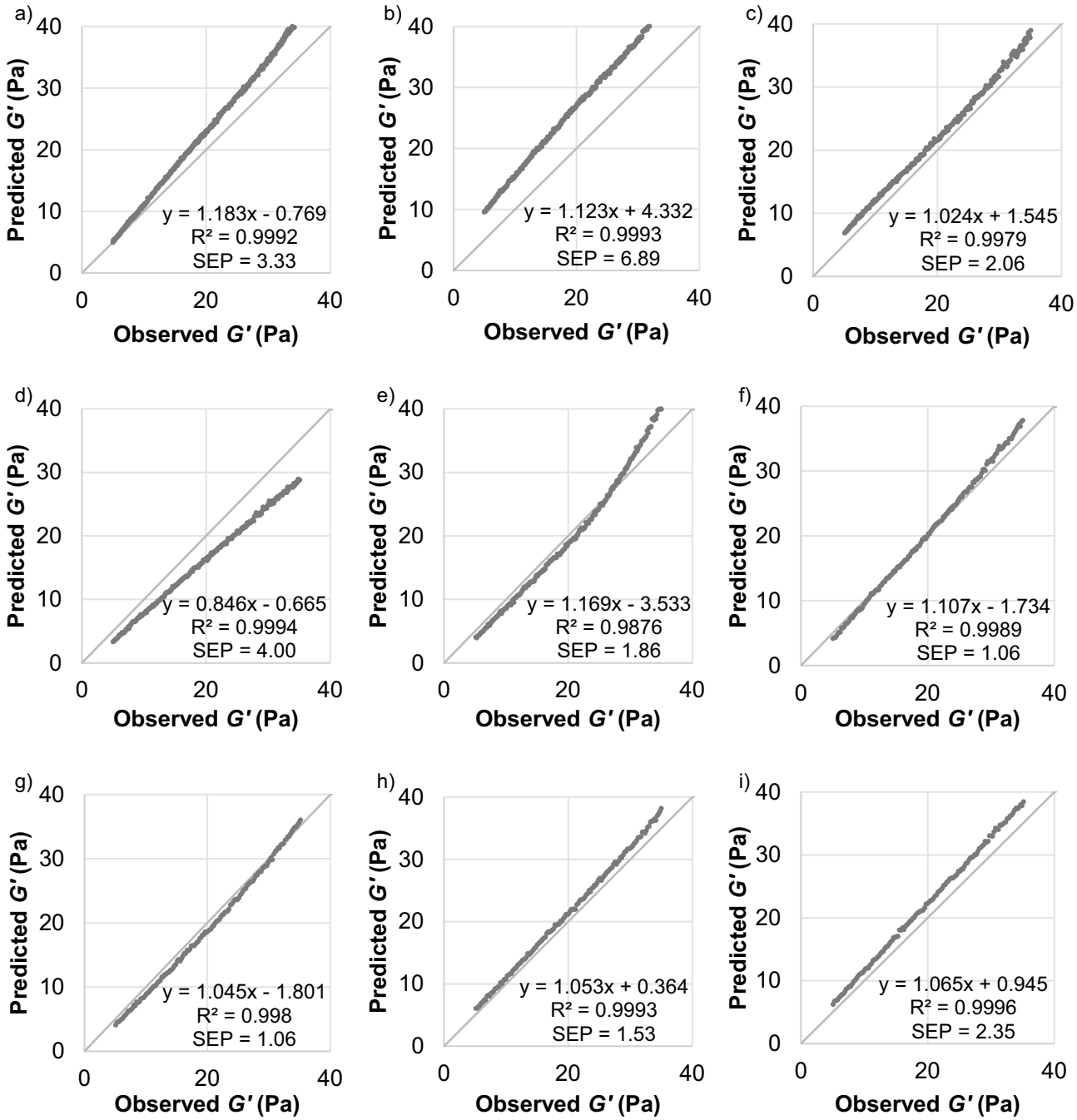

Fig. 7 Validation of the storage modulus (G') prediction model using a 600 µm multifiber probe at 780 nm, at different protein and $CaCl_2$ levels: a) 3.2% and 150 mg L^{-1} (N = 388); b) 3.2% and 200 mg L^{-1} (N = 322); c) 3.2% and 250 mg L^{-1} (N = 277); d) 3.6% and 150 mg L^{-1} (N = 235); e) 3.6% and 200 mg L^{-1} (N = 206); f) 3.6% and 250 mg L^{-1} (N = 154); g) 4.0% and 150 mg L^{-1} (N = 141); h) 4.0% and 200 mg L^{-1} (N = 137); i) 4.0% and 250 mg L^{-1} (N = 130). Validation data corresponding to the replication of the curve R *vs* time closest to the average (see "Statistical Analysis" section). N, Number of validation datapoints; R^2, coefficient of determination; SEP, standard error of prediction (Pa)

G' = 30 Pa, which can be considered an excellent fit according to the criteria of (Malley et al., 2005).

When the model was validated with the curve R *vs* time replication closest to the average of the three replications, the fit improved substantially (Table 8). In this case, the ranges of SEP and CV values were 1.06–6.89 Pa and 5.3–34.4%, representing an average improvement of 60.5 and 60.3% for each of them, respectively, compared to the initial calibration procedure. At 3.2 and 3.6% protein concentrations, addition of 250 mg L^{-1} $CaCl_2$ yielded better models than with

lower amounts, obtaining SEP values of 2.06 and 1.06 for each protein concentration, respectively (Fig. 7c–f)). On the contrary, validation at 4.0% protein got worse as the amount of added calcium increased but their SEP values ranged from 1.06 to 2.35 Pa showing that at the highest level of protein concentration, accurate predictions of *G'* were obtained with the three levels of calcium evaluated (Fig. 7g–i).

Conclusions

Using a multifiber probe with a core size of 600 µm at a wavelength of 780 nm allowed obtaining a better optical response of the sensor during enzymatic coagulation of milk than a 400 µm probe. It showed greater sensitivity to variations in protein and fat content of the milk and lower variation in the response. The 600 µm multifiber probe at a wavelength of 780 nm generated a NIR light backscatter profile like those obtained with other devices, thus, the usual optical parameters containing information regarding the different coagulation phases of milk coagulation could be determined. The elastic modulus (*G'*) prediction model proposed in previous works was successfully validated (SEP < 7 Pa) with the selected multifiber probe. Thus, tested multifiber probes are low cost, which would facilitate the implementation of the optical system at an industrial level for inline prediction of G´. In parallel, the results of the present study showed that the parameters of the prediction model had an approximately linear variation as a function of the two main factors studied (i.e., protein and calcium), which opens the possibility to substantially improve the performance of the prediction model. The addition of calcium accelerated the hydrolysis, gelation and firming phases of the curd. It was attributed to the increase of ionic and colloidal calcium and subsequent pH diminution, which generated a reduction in the electrostatic repulsion between the casein micelles and accelerated gelation. Furthermore, the initial voltage obtained with the probe responded linearly to the different protein levels in milk. This fact would make possible, at least theoretically, to estimate protein concentration with the same *inline* probe for *G'* determination, facilitating the incorporation of a corrective protein factor in the prediction models, using a single instrument.

Author Contributions Zulma Villaquiran: investigation, writing- original draft, formal analysis, data curation. Ana Zamora: conceptualization, methodology, formal analysis, editing. Oscar Arango: conceptualization, writing- original draft, formal analysis, writing-review. Manuel Castillo: conceptualization, methodology, formal analysis, writing-review.

Funding Open Access Funding provided by Universitat Autonoma de Barcelona. Proof of Concept 2018 funded by the Valorisation and Patents Office at the Universitat Autònoma de Barcelona.

Data Availability Data are available on request.

Declarations

Competing Interests The authors declare no competing interests.

References

Arango, O., & Castillo, M. (2018). A method for the inline measurement of milk gel firmness using an optical sensor. *Journal of Dairy Science, 101*(5), 3910–3917. https://doi.org/10.3168/jds.2017-13595

Arango, O., Trujillo, A. J., & Castillo, M. (2015). Predicting coagulation and syneresis parameters of milk gels when inulin is added as fat substitute using infrared light backscatter. *Journal of Food Engineering, 157*, 63–69. https://doi.org/10.1016/j.jfoodeng.2015.02.021

Arango, O., Trujillo, A. J., & Castillo, M. (2018a). Modelling gelation and cutting times using light backscatter parameters at different levels of inulin, protein and calcium. *LWT - Food Science and Technology, 91*, 505–510. https://doi.org/10.1016/j.lwt.2018.01.081

Arango, O., Trujillo, A. J., & Castillo, M. (2018b). Monitoring the effect of inulin, protein, and calcium on milk coagulation phases using a fibre optic sensor. *International Dairy Journal, 81*, 80–86. https://doi.org/10.1016/j.idairyj.2018.01.015

Castillo, M. (2006). Cutting time prediction methods in cheese making. *Encyclopedia of Agricultural, Food, and Biological Engineering, 1*, 1–7. https://doi.org/10.1081/E-EAFE-120040365

Castillo, M., & Arango, O. (2018). *A method and a system for determining gel firmness values from inline optical measurements* (Patent No. EP3036527 B1).

Castillo, M., Payne, F. A., Hicks, C. L., Laencina, J. S., & López, M. B. M. (2003). Modelling casein aggregation and curd firming in goats' milk from backscatter of infrared light. *Journal of Dairy Research, 70*(3), 335–348. https://doi.org/10.1017/S0022029903006356

Castillo, M., Payne, F. A., López, M. B., Ferrandini, E., & Laencina, J. (2005). Optical sensor technology for measuring whey fat concentration in cheese making. *Journal of Food Engineering, 71*(4), 354–360. https://doi.org/10.1016/j.jfoodeng.2004.10.046

Fagan, C. C., Castillo, M., Payne, F. A., Donnell, C. P. O., & Callaghan, D. J. O. (2007). Effect of cutting time, temperature, and calcium on curd moisture, whey fat losses, and curd yield by response surface methodology. *Journal of Dairy Science, 90*(10), 4499–4512. https://doi.org/10.3168/jds.2007-0329

Fox, P. F., Guineee, T. P., Cogann, T. M., & McSweeney, P. L. H. (2017). *Fundamentals of Cheese Science* (2nd ed.). Springer. https://doi.org/10.1007/978-1-4899-7681-9

Lewis, M. J. (2011). The measurement and significance of ionic calcium in milk - A review. *International Journal of Dairy Technology, 64*(1), 1–13. https://doi.org/10.1111/j.1471-0307.2010.00639.x

Lin, M. J., Lewis, M. J., & Grandison, A. S. (2006). Measurement of ionic calcium in milk. *International Journal of Dairy Technology, 59*(3), 192–199. https://doi.org/10.1111/j.1471-0307.2006.00263.x

Malley, D. F., McClure, C., Martin, P. D., Buckley, K., & McCaughey, W. P. (2005). Compositional analysis of cattle manure during composting using a field-portable near-infrared spectrometer. *Communications in Soil Science and Plant Analysis, 36*(4–6), 455–475. https://doi.org/10.1081/CSS-200043187

Nicolau, N., Buffa, M., O'Callaghan, D. J., Guamis, B., & Castillo, M. (2015). Estimation of clotting and cutting times in sheep cheese manufacture using NIR light backscatter. *Dairy Science and Technology, 95*(4), 495–507. https://doi.org/10.1007/s13594-015-0232-7

O'Callaghan, D. J., & O'Donnell, C. P. (2022). Monitoring gel formation in cheese manufacture. In P. L. H. McSweeney & J. P. McNamara (Eds.), *Encyclopedia of Dairy Sciences* (3rd ed., pp. 238–244). Academic Press. https://doi.org/10.1016/B978-0-12-818766-1.00200-2

Payne, F. A., & Castillo, M. (2007). Light backscatter sensor applications in milk coagulation. In D. Heldman (Ed.), *Encyclopedia of Agricultural, Food, and Biological Engineering* (1st ed., Vol. 1, pp. 1–5). Taylor & Francis Group. https://doi.org/10.1081/E-EAFE-120042609

Salvador, D., Arango, O., & Castillo, M. (2019). In-line estimation of the elastic module of milk gels with variation of temperature protein concentration. *International Journal of Food Science and Technology, 54*(2), 354–360. https://doi.org/10.1111/ijfs.13944

Sandra, S., Ho, M., Alexander, M., & Corredig, M. (2012). Effect of soluble calcium on the renneting properties of casein micelles as measured by rheology and diffusing wave spectroscopy. *Journal of Dairy Science, 95*(1), 75–82. https://doi.org/10.3168/jds.2011-4713

Utzinger, U., & Richards-Kortum, R. R. (2003). Fiber optic probes for biomedical optical spectroscopy. *Journal of Biomedical Optics, 8*(1), 121–147. https://doi.org/10.1117/1.1528207

Walstra, P., Wouters, J. T. M., & Geurts, T. J. (2006). *Dairy science and technology* (2nd ed.). CRC Press. https://doi.org/10.1201/9781420028010

Woodcock, T., Fagan, C. C., O'Donnell, C. P., & Downey, G. (2008). Application of near and mid-infrared spectroscopy to determine cheese quality and authenticity. *Food and Bioprocess Technology, 1*(2), 117–129. https://doi.org/10.1007/s11947-007-0033-y

Xie, D., & Guo, W. (2020). Measurement and calculation methods on absorption and scattering properties of turbid food in Vis/NIR Range. *Food and Bioprocess Technology, 13*(2), 229–244. https://doi.org/10.1007/s11947-020-02402-3